

Published in final edited form as:

*Clin Cancer Res.* 2013 September 15; 19(18): . doi:10.1158/1078-0432.CCR-13-0551.

## Tumor-infiltrating lymphocytes in glioblastoma are associated with specific genomic alterations and related to transcriptional class

W. Caleb Rutledge<sup>1</sup>, Jun Kong<sup>2,3</sup>, Jingjing Gao<sup>2,3</sup>, David A. Gutman<sup>2,3</sup>, Lee A.D. Cooper<sup>2,3</sup>, Christina Appin<sup>4</sup>, Yuna Park<sup>4</sup>, Lisa Scarpace<sup>6</sup>, Tom Mikkelsen<sup>6</sup>, Mark L. Cohen<sup>7</sup>, Kenneth D. Aldape<sup>8</sup>, Roger E. McLendon<sup>9</sup>, Norman L. Lehman<sup>10</sup>, C. Ryan Miller<sup>11</sup>, Matthew J. Schniederjan<sup>12</sup>, Cameron W. Brennan<sup>13</sup>, Joel H. Saltz<sup>2,3,4</sup>, Carlos S. Moreno<sup>2,3,4</sup>, and Daniel J. Brat<sup>2,3,4</sup>

<sup>1</sup>Emory University School of Medicine, Atlanta, GA

<sup>2</sup>Department of Biomedical Informatics, Emory University, Atlanta, GA

<sup>3</sup>Center for Comprehensive Informatics, Emory University, Atlanta, GA

<sup>4</sup>Department of Pathology and Laboratory Medicine, Emory University, Atlanta, GA

<sup>5</sup>Winship Cancer Institute, Emory University, Atlanta, GA

<sup>6</sup>Department of Neurosurgery, Henry Ford Hospital, Detroit, MI

<sup>7</sup>Department of Pathology, Case Western Reserve University, Cleveland, OH

<sup>8</sup>Department of Pathology, University of Texas MD Anderson Cancer Center, Houston, TX

<sup>9</sup>Department of Pathology, Duke University Medical Center, Durham, NC

<sup>10</sup>Department of Pathology, Ohio State University, Columbus OH

<sup>11</sup>Department of Pathology, University of North Carolina, Chapel Hill, NC

<sup>12</sup>Department of Pathology, Children's Healthcare of Atlanta, Atlanta, GA

<sup>13</sup>Department of Neurosurgery, Memorial Sloan Kettering Cancer Center, New York, NY

### Abstract

**Purpose**—Tumor-infiltrating lymphocytes (TILs) have prognostic significance in many cancers, yet their roles in glioblastoma (GBM) have not been fully defined. We hypothesized TILs in GBM are associated with molecular alterations, histologies and survival.

**Experimental Design**—We used data from The Cancer Genome Atlas (TCGA) to investigate molecular, histologic and clinical correlates of TILs in GBMs. Lymphocytes were categorized as absent, present or abundant in histopathologic images from 171 TCGA GBMs. Associations were examined between lymphocytes and histologic features, mutations, copy number alterations, CpG island methylator phenotype, transcriptional class and survival. We validated histologic findings using *CD3G* gene expression.

**Results**—We found a positive correlation between TILs and GBMs with gemistocytes, sarcomatous cells, epithelioid cells and giant cells. Lymphocytes were enriched in the

---

**Corresponding Author:** Daniel J. Brat, M.D., Ph.D., Department of Pathology and Laboratory Medicine, Emory University Hospital, G-167, 1364 Clifton Road NE, Atlanta, GA 30322, Phone: 404-712-1266, Fax: 404-727-3133, dbrat@emory.edu.

**Conflict of interest:** The authors have no conflicts of interest.

mesenchymal transcriptional class and strongly associated with mutations in *NFI* and *RBI*. These mutations are frequent in the mesenchymal class and characteristic of gemistocytic, sarcomatous, epithelioid and giant cell histologies. Conversely, TILs were rare in GBMs with small cells and oligodendroglioma components. Lymphocytes were depleted in the classical transcriptional class and in *EGFR*-amplified and homozygous *PTEN*-deleted GBMs. These alterations are characteristic of GBMs with small cells and GBMs of the classical transcriptional class. No association with survival was demonstrated.

**Conclusions**—TILs were enriched in GBMs of the mesenchymal class, strongly associated with mutations in *NFI* and *RBI* and typical of histologies characterized by these mutations. Conversely, TILs were depleted in the classical class, *EGFR*-amplified and homozygous *PTEN*-deleted tumors and rare in histologies characterized by these alterations.

### Keywords

Glioblastoma; Lymphocytes; The Cancer Genome Atlas; Transcriptional class; Mesenchymal; Classical; Neurofibromatosis 1 (*NFI*); Retinoblastoma 1 (*RBI*); Epidermal growth factor receptor (*EGFR*); Tumor protein 53 (*TP53*); Phosphatase and tensin homolog (*PTEN*)

## INTRODUCTION

Glioblastoma (GBM) is the most common and highest grade astrocytoma (World Health Organization, grade IV). Despite advances in diagnosis and treatment, GBM remains incurable with an average survival of 15 months.(1) Although characterized by dramatic molecular and histologic heterogeneity, current adjuvant treatments inhibit cell division nonspecifically and are not tailored to specific subsets.(1, 2) Molecular classifications of GBM have revealed distinct subclasses with clinical relevance, opening the way for therapies to be directed at class-specific mechanisms.(3, 4) Immunotherapy, for example, has great potential as a tailored therapy. Already FDA-approved for prostate cancer and metastatic melanoma and in clinical trials for other cancer types, immunotherapy remains promising for patients with GBM, offering high tumor-specificity and long-term tumor surveillance.(5–7)

Tumor-infiltrating lymphocytes (TILs) are present in subsets of GBM, yet their biologic activities and clinical relevance have not been fully explored. The presence of TILs suggests an anti-tumor adaptive immune response and might be expected to impact survival. Lymphocytes are present within the stroma of other cancers, including melanoma, colorectal and ovarian carcinoma, where their presence is associated with improved patient outcomes. (8–17) A recent study suggested TILs have prognostic significance in GBM, yet others have shown lymphocytes may impart a less favorable prognosis.(18–21)

A complex relationship exists between the development of cancer, the immunologic response to it and the immunosuppression it causes. In GBM, tumor-mediated immunosuppression is thought to explain functional deficits in cytotoxic lymphocytes.(22) Regulatory lymphocytes are elevated in patients with GBM and suppress anti-tumor activity by inhibiting secretion of cytotoxic cytokines from effector lymphocytes.(23, 24) Thus, while lymphocytes and other immune cells infiltrate GBM, an immunosuppressive tumor milieu likely prevents successful immune-mediated tumor eradication. Recent clinical trials have focused on augmenting the anti-tumor immune response with tumor vaccines or reversing tumor-mediated immunosuppression.

Molecular alterations in GBM and other cancers may be immunogenic. For example, microsatellite instability and methylation aberrations are independent predictors of lymphocyte density in colorectal cancer.(14) Given its molecular and histologic

heterogeneity, subsets of GBM may be more immunogenic and responsive to immunotherapy, yet little is known about the relation between immune cells and the tumor microenvironment or molecular classes in GBM. Therefore, the purpose of this study was to identify molecular and histologic correlates of the immune response in GBM. We used whole-slide digitized images of GBMs from The Cancer Genome Atlas (TCGA) linked to multiplatform molecular data. These may provide insight into the biologic significance of TILs in GBM and impact therapy.

## MATERIALS AND METHODS

We performed an integrated molecular and histologic analysis using data from TCGA, which molecularly characterized GBMs across multiple platforms, including single-nucleotide polymorphism (SNP) genotyping, mRNA and microRNA profiling, DNA sequencing and methylation analysis.<sup>(2)</sup> Clinical data, including treatment and survival, is also available.

### Digitized Images used for Morphological Analysis

Permanent section histologic slides from TCGA GBMs were provided by contributing institutions. Slides were scanned and digitized at 20X resolution by a high-throughput digital scanner (Aperio, Inc.) at the TCGA Biospecimen Core Resource located at the International Genomics Consortium (Intgen, Phoenix, AZ). The number of slides available for review ranged from 1–9 per case (median, 3).

### Ratings of TILs and other Histopathologic Features

TCGA consortium neuropathologists annotated digitized permanent section histologic slides from 122 TCGA cases for 18 histopathologic features, including inflammation, angiogenesis, necrosis, lymphocytes, common morphologic subtypes and others (Table 1). “Inflammation” as a general category was defined by the presence of inflammatory cells, including lymphocytes, macrophage, neutrophils or their combination. Lymphocytes were identified as small round cells with scant cytoplasm and darkly staining nuclei. Lymphocytes and all other histopathologic features were categorized as absent (0), present (1+) or abundant (2+) by two neuropathologists (MC, KA, RM, NL, RM, MJS, DJB) and adjudicated by a third. Cases with a complete absence of lymphocytes were labeled 0 (absent). Cases with lymphocytes in <50% of tumor tissue were categorized 1+ (present), while cases with lymphocytes in ≥50% were categorized 2+ (abundant) (Figure 1). In addition to these 122 cases, an additional 49 TCGA cases from Emory University Hospital and Henry Ford Health System were annotated for the same 18 histopathologic features using the same criteria by two TCGA neuropathologists (DJB, MJS). All digitized histologic sections and TCGA neuropathology ratings were obtained from the TCGA portal (<http://tcga-data.nci.nih.gov.proxy.library.emory.edu/tcga/tcgaHome2.jsp>; last accessed November 28, 2012). Digitized images and corresponding neuropathology ratings were the primary source of data.

### Mutations, Copy Number Alterations, Methylation Status and Transcriptional Class

We obtained TCGA mutation and copy number data from the Memorial Sloan Kettering Cancer Genomics Portal (<http://www.cbioportal.org/public-portal>; last accessed November 28, 2012).<sup>(25)</sup> Mutation data from whole exome sequencing (NextGen) was obtained for 99 cases. Putative copy-number calls determined with GISTIC 2.0 were obtained for 153 cases. CpG island methylator phenotype (G-CIMP) status was available for 124 cases. Transcriptional class labels for the Verhaak classification were obtained for 162 cases from the TCGA Advanced Working Group. The updated Verhaak labeling extends the original

labeled set presented in Verhaak *et al.* by using the originally labeled samples along with Affymetrix HT\_HG-U133A data to label previously unclassified samples.(3)

### Validation Dataset

*CD3G* is the gene that encodes the T-cell surface marker CD3. We used *CD3G* expression data from TCGA as a marker of lymphocytes to validate our histologic findings in the same set of tumors. *CD3G* expression data was obtained from the TCGA portal (<http://tcga-data.nci.nih.gov.proxy.library.emory.edu/tcga/tcgaHome2.jsp>; last accessed February 1, 2012).

### Statistical Analyses

Associations between lymphocytes and other histopathologic features were assessed using the Mantel-Haenzel chi-square and exact test and Spearman correlation for ordinal comparisons (0, 1+, 2+ vs 0, 1+, 2+). The Mantel-Haenzel exact test was used when the cell count was <5 in 25% or more of cells. Chi-square and Fisher's exact test were used for all dichotomous comparisons (0 vs 1+, 2+ combined or 0, 1+ combined vs 2+). We combined categories to identify associations driven by cases with either complete absence or abundance of lymphocytes. The association of lymphocytes with mutations, copy number alterations and G-CIMP status were also assessed using chi-square and Fisher's exact test. Fisher's exact test was used when the cell count was <5 in 25% or more of cells. Associations between lymphocytes and transcriptional class were examined using chi-square and Fisher's exact test. The Spearman correlation was used to measure the correlation between lymphocytes and *CD3G* expression. Wilcoxon two-sample or Kruskal-Wallis tests were used to detect differences in *CD3G* expression according to lymphocytes, mutation or copy number status and transcriptional class.

### Survival Analysis

Clinical data was obtained from the TCGA data portal. Survival was taken as "days to death" for uncensored patients and "days to last follow-up" for right-censored patients. The association between TILs and survival was examined using the log-rank test.

All p-values reported are two-sided and regarded as statistically significant if  $p < 0.05$ . The software used for statistical analysis was SAS Version 9.3 (SAS Institute Inc., Cary NC).

## RESULTS

### TILs are differentially distributed in GBM

Within the 171 GBMs reviewed for this study, tumor-infiltrating lymphocytes (TILs) were absent (0) in 93 cases (54%), present (1+) in 59 cases (35%) and abundant (2+) in 19 cases (11%). There was no significant association between the number of slides analyzed for each case and the level of lymphocytes annotated.

### TILs are associated with specific histopathologic features in GBM

GBMs show a tremendous degree of histologic variability and numerous morphologic subtypes have been recognized, including fibrillary, gemistocytic, epithelioid, small cell, giant cell, gliosarcoma and GBM with oligodendroglioma component. To determine if TILs correlated with specific GBM morphologies or other histopathologic features, we examined their associations using the Mantel-Haenzel chi-square test and Spearman correlation (Table 1). All variables, including lymphocytes and other histopathologic features were categorized as 0, 1+ or 2+. We detected a strong positive correlation between TILs and specific tumor cell morphologies that included gemistocytes, sarcomatous cells, epithelioid cells and giant

cells (all  $p < 0.05$ ) (Figure 2). Conversely, TILs were depleted in GBMs characterized by small cells and oligodendroglial cells (both  $p < 0.05$ ). Among other features analyzed, TILs were most tightly correlated with the findings of inflammation (as a general category) and macrophages (both  $p < 0.05$ ). TILs were also statistically associated with both forms of necrosis annotated (pseudopalisading and zonal) (both  $p < 0.05$ ).

### TILs are associated with specific mutations in GBM

In the initial TCGA analysis of GBM, eight genes were identified as significantly mutated, including *TP53*, *PTEN*, *NF1*, *EGFR*, *ERBB2*, *RBI*, *PIK3RI* and *PIK3CA* (genes attaining a false discovery rate  $< 0.1$ ).<sup>(2)</sup> A subsequent, unbiased genomic analysis identified recurrent mutations in isocitrate dehydrogenase 1 (*IDH1*).<sup>(26)</sup> We examined associations between lymphocytes (0, 1+, 2+) and mutations (mutant vs wild type) for these genes using chi-square and Fisher's exact test (Table 2). Our data set contained no cases with *ERBB2* mutations.

Among cases with mutational data, lymphocytes were absent (0) in 52, present (1+) in 38 and abundant (2+) in 9. We found lymphocytes were strongly associated with mutations in neurofibromatosis 1 (*NF1*) and retinoblastoma 1 (*RBI*) (both  $p < 0.05$ ). Nine cases with absent (0) lymphocytes were *NF1*-mutant (9/52, 17%), while 44% of cases with abundant (2+) lymphocytes harbored mutations in *NF1* (4/9). Two cases with absent (0) lymphocytes harbored mutations in *RBI* (2/52, 4%). Of cases with lymphocytes present (1+), six were *RBI* mutants (6/32, 16%). Two cases with abundant (2+) lymphocytes harbored mutations in *RBI* (2/9, 22%).

There was a trend towards significance for *TP53* mutations ( $p = 0.12$ ), particularly when cases with present (1+) and abundant (2+) lymphocytes were combined ( $p = 0.06$ ). 25% of cases with absent (0) lymphocytes were *TP53*-mutant (13/52), while 43% of cases with present (1+) or abundant (2+) lymphocytes harbored mutations in *TP53* (20/47).

Since mutations in *TP53* are characteristic of both the proneural and mesenchymal transcriptional class, we investigated if mutations were overrepresented in one of these two transcriptional classes.<sup>(3)</sup> 20 cases harbored mutations in *TP53* and had present (1+) or abundant (2+) lymphocytes. Nine (45%) belonged to the mesenchymal transcriptional class and five (25%) belonged to the proneural class ( $p > 0.05$ ).

### TILs are associated with specific copy number alterations in GBM

Significant copy number alterations (CNAs) were also identified in the initial TCGA global analysis publication, including amplifications of *EGFR*, *CDK4*, *PDGFRA*, *MDM2*, *MDM4*, *MET*, *CDK6*, *MYCN*, *CCND2*, *PIK3CA* and *AKT3* and deletions of *CDKN2A/B*, *PTEN*, *CDKN2C*, *RBI*, *PARK2* and *NF1*.<sup>(2)</sup> We examined the association between TILs and these recurrent amplifications and deletions using chi-square and Fisher's exact test (Table 3). Lymphocytes were depleted in *EGFR*-amplified tumors ( $p < 0.05$ ). Amplification of *EGFR* was present in 65% of cases with absent (0) lymphocytes (53/82) compared to 48% of cases with present (1+) or abundant (2+) lymphocytes. Only 35% of cases with abundant (2+) lymphocytes were *EGFR*-amplified.

TILs were also depleted in tumors with homozygous deletions of *PTEN* ( $p < 0.05$ ). 78% of cases with homozygous *PTEN*-deletion (14/18) had absent (0) lymphocytes. 17% of *PTEN*-deleted cases had present (1+) lymphocytes (3/18), while only 5% of cases had abundant (2+) lymphocytes (1/18). There was a trend towards significance for *NF1* deletions ( $p = 0.07$ ). No other associations between TILs and copy number alterations were noted.

### TILs are not associated with the CpG island methylator phenotype

G-CIMP positive tumors represent less than 10% of GBMs, but have significantly improved survival compared to G-CIMP negative tumors.(27) *IDH1* mutations have been shown to establish the G-CIMP phenotype.(28) We examined the association between TILs and the CpG island methylator phenotype using chi-square and Fisher's exact test (data not shown). TILs were not associated with G-CIMP status ( $p>0.05$ ).

### TILs are related to transcriptional class

Verhaak *et al.* identified four transcriptional classes of GBM using TCGA gene expression data: proneural, neural, classical and mesenchymal.(3) To determine if there was an association between transcriptional class and TILs, we examined each class for its distribution of lymphocytes using chi-square and Fisher's exact test (Table 4). We found TILs were strongly associated with transcriptional class ( $p<0.05$ ).

TILs were enriched in the mesenchymal class compared to all other classes combined ( $p<0.05$ ). 42% of cases (30/72) with a lymphocytic infiltrate (1+ or 2+) belonged to the mesenchymal class. However, when classical tumors were excluded, there was no statistically significant enrichment of TILs in the mesenchymal class compared to the proneural and neural classes ( $p>0.05$ ). Cases with abundant lymphocytes were heavily enriched in mesenchymal transcriptional class. 71% of cases (12/17) with abundant lymphocytes (2+) belonged to the mesenchymal class, whereas 12% were proneural, 12% neural and 6% were classical, representing statistically significant enrichment ( $p<0.05$ ). When classical cases were excluded, there was a still a strong trend towards statistically significant enrichment of abundant (2+) TILs in the mesenchymal class compared to the proneural and neural classes ( $p=0.07$ ).

Conversely, TILs were depleted in the classical transcriptional case compared to all other classes combined ( $p<0.05$ ). 74% of classical cases (31/42) were characterized by absent (0) lymphocytes, representing statistically significant depletion ( $p<0.05$ ). Only one case with abundant (2+) lymphocytes belonged to the classical transcriptional class (1/17). When mesenchymal tumors were excluded, there was still a trend towards statistically significant depletion of TILs (1+ and 2+) in the classical class compared to the proneural and neural classes ( $p=0.053$ ).

### ***CD3G* gene expression is positively correlated with lymphocytes, mutations in *TP53*, *RB1* and the mesenchymal transcriptional class and negatively correlated with *EGFR* amplification, *PTEN* deletion and the classical transcriptional class**

We used *CD3G* expression data to validate findings uncovered by our morphologic analysis. There was a positive correlation (0.30) between the histologic categorization of lymphocytes and *CD3G* expression ( $p<0.001$ ). GBMs with higher levels of TILs had significantly higher *CD3G* expression ( $p<0.001$ ). Those with absent (0), present (1+) and abundant (2+) lymphocytes had *CD3G* expression of 15.34 (Standard deviation (SD)  $\pm$  7.81), 17.55 (SD  $\pm$  10.99) and 20.23 (SD  $\pm$  13.51), respectively

We examined levels of *CD3G* expression in cases harboring mutations in *RB1*, *TP53* and *NF1*. Cases with *RB1* mutations tended to have higher levels of *CD3G* expression than wild type cases (19.1 vs 16.2). Cases with *TP53* mutations also showed higher levels of *CD3G* expression than wild type (17.4 vs 16.0). Cases with *NF1* mutations had lower levels of *CD3G* expression compared to wild type (15.6 vs 16.5) (all  $p>0.05$ ).

We also investigated *CD3G* expression in *EGFR*-amplified and *PTEN*-deleted cases. *EGFR*-amplified cases had lower levels of *CD3G* expression than wild type (15.6 vs 16.7).

Likewise, *PTEN*-deleted cases also had lower levels of *CD3G* expression (15.5 vs 16.3) (both  $p > 0.05$ ).

Finally, we analyzed *CD3G* expression levels by transcriptional class. There was a statistically significant difference in expression according to transcriptional class ( $p < 0.001$ ). Cases belonging to the mesenchymal transcriptional class had the highest *CD3G* expression (19.6), which was significantly higher than that of other classes combined (15.1) ( $p < 0.001$ ). Conversely, *CD3G* expression was significantly lower in the classical transcriptional class compared to all other classes (14.8 vs 17.1) ( $p < 0.001$ ).

### TILs are not associated with prolonged with survival

TILs were not associated with prolonged survival in univariate analyses. We compared the survival of cases with absent (0) lymphocytes, present (1+) and abundant (2+) lymphocytes using a log-rank test ( $p > 0.05$ ) (Figure 3). We found patient age was a highly significant predictor of survival ( $p < 0.001$ ); however, lymphocytes did not vary according to age. The mean age of patients with absent (0), present (1+) and abundant (2+) lymphocytes was 56.9 (SD  $\pm$  14.6), 57.3 (SD  $\pm$  12.1) and 54.8 years (SD  $\pm$  13.1), respectively ( $p > 0.05$ ). TILs were not a significant predictor of survival in an age-adjusted Cox proportional hazards model (data not shown) ( $p > 0.05$ ). If tumors belonging to the classical transcriptional class were excluded, there were no survival differences according to TILs among proneural, neural and mesenchymal tumors ( $p > 0.05$ ). Similarly, if mesenchymal tumors were excluded, there were no survival differences according to TILs among proneural, neural and classical tumors ( $p > 0.05$ ).

## DISCUSSION

Lymphocytes are present in the stroma of many human cancers. The histologic finding of tumor-infiltrating lymphocytes (TILs) is often associated with prolonged survival. Tumors with TILs may have distinctive clinicopathologic features or underlying genetic alterations, which could be relevant for future tailored therapies.

Although prognostically significant in other cancers, the clinical relevance and genetic associations of TILs in GBM remains unclear. The TCGA data set offers an opportunity to study the relationship between morphologic features, molecular alterations and survival in GBM.(3, 4) Verhaak *et al.* used TCGA gene expression profiles to identify four transcriptional classes, while independent studies of genome methylation uncovered a hypermethylated, G-CIMP+ subset characterized by IDH mutations and overproduction of the oncometabolite 2-hydroxyglutarate (2-HG).(3, 26, 29) Recent evidence suggests GBMs within the mesenchymal transcriptional class have a better response to immunotherapy, suggesting this class may be more immunogenic.(30) We hypothesized TILs are differentially distributed within specific morphologic and molecular classes of GBM.

We found TILs were not uniformly distributed among GBMs, suggesting some are more capable of eliciting an immune response. Indeed, lymphocytes were absent in over half, as determined morphologically by a panel of TCGA neuropathologists. TILs were strongly enriched in the mesenchymal transcriptional class of GBM, which suggests tumors belonging to this subtype are more immunogenic. Seventy-one percent of tumors with abundant (2+) lymphocytes belonged to the mesenchymal class. No other transcriptional class had more than 12% with abundant (2+) TILs, indicating a fundamental difference in transcriptional class with regard to TILs.

Variation of TILs could potentially be accounted for by the extent of necrosis, since the mesenchymal class signature is heavily influenced by the degree of necrosis and the

presence of lymphocytes was associated with necrosis in this study.(31) However, mesenchymal GBMs with abundant (2+) TILs did not have substantially different levels of necrosis than those with no TILs. Neither zonal or pseudopalisading necrosis were associated with transcriptional class. Moreover, molecular alterations associated with the mesenchymal class are more likely to be responsible for the association with TILs. Lymphocytes were strongly associated with mutations in *NF1* and *RB1* and a trend was noted for *TP53* mutations. Mutations of *NF1* and *RB1* are characteristic of the mesenchymal transcriptional class and *TP53* mutations are common in both the mesenchymal and proneural subtypes. Interestingly, we found *TP53* mutant tumors with abundant (2+) TILs were more common in the mesenchymal than the proneural class, but this did not reach statistical significance.

We also found TILs were more common in certain morphologic subsets of GBM, including those with sarcomatous, giant cell, epithelioid and gemistocytic components. This was of interest since prior studies have shown gliosarcoma, giant cell glioblastoma and gemistocytic astrocytomas are all characterized by a high frequency of *TP53* mutations.(32–34) Our own studies using TCGA data indicated sarcomatous components in GBM were associated with *NF1*, *RB1* and *TP53* mutations; giant cells were associated with *TP53* and *RB1* mutations; and epithelioid cells were associated with *NF1* and *RB1* mutations (data not shown). We did not find an association between *TP53* mutations and gemistocytic cells, likely because of inclusion of tumors with low levels of this histologic finding as compared to prior studies, which included morphologically pure gemistocytic astrocytomas of lower grade. Nonetheless, we found the presence of TILs was strongly associated with the mesenchymal transcriptional class as well as the mutations and tumor morphologies associated with this gene signature.

We also found TILs were rare in tumors of the classical transcriptional class, suggesting these may exclude lymphocytes and prevent immune-mediated tumor eradication. Only one case with abundant (2+) lymphocytes belonged to the classical transcriptional class (1/17). We also noted TILs were depleted in *EGFR*-amplified GBMs, which are frequent in the classical transcriptional class of GBMs, but less common in other classes, including mesenchymal. Since small cell GBMs have been shown to have a high frequency *EGFR* amplification, we were also encouraged that the histologic presence of small cells within GBMs from the TCGA data set was associated with TIL depletion.(35) Recent evidence suggests *EGFR* activation may repress the adaptive immune response, potentially through attenuation of MHC I and MHC II expression, and therefore explain the relation between *EGFR* amplification and lymphocyte depletion.(36) We also found TILs were depleted in *PTEN*-deleted tumors (homozygous). Loss of *PTEN* has been shown to increase expression of the immunosuppressive protein B7 homolog 1 (B7-H1), and therefore may account for the association between homozygous *PTEN* deletion and lymphocyte depletion.(22)

We used *CD3G* expression data from TCGA to validate our morphologic findings. The *CD3G* gene encodes a protein that forms the T cell receptor-CD3 complex and is highly specific to T lymphocytes and present in all subsets. The correlation between lymphocytes and *CD3G* expression was highly statistically significant ( $p < 0.001$ ), however the strength of the correlation was moderate (0.3). Although the tissue used for molecular analysis by TCGA was from the same neoplasm as the tissue used to create slide images, the distribution of TILs in tumors can be irregular and may contribute to a weak correlation. In addition, the detection and evaluation of TILs by molecular and pathologic methods differ considerably and may also lead to a weakened correlation. However, we were encouraged that mutations associated with TILs (*RB1* and *TP53*) tended to have higher levels of *CD3G* expression, whereas copy number alterations associated with depletion of lymphocytes (*EGFR* amplification and homozygous *PTEN* deletion) had lower *CD3G* expression.



Tumors of the mesenchymal transcriptional class had significantly higher *CD3G* expression than all other subtypes, while those of the classical subtype had significantly lower expression, which corroborates the associations uncovered in our morphologic analysis.

GBMs annotated as having zonal necrosis by TCGA neuropathologists did not have significantly higher levels of *CD3G* expression and those with pseudopalisading necrosis had lower levels of *CD3G* expression, suggesting TILs may indeed represent an anti-tumor adaptive immune response rather than a response to necrosis.

In summary, our analysis of digitized, whole slide H&E-stained images from TCGA had the advantage of a large number of cases and high quality, multi-platform molecular analysis. It illustrates the power of networks such as the TCGA to link multi-platform molecular analysis to histopathologic findings in cancer with implications for future therapy. The categorical classification of lymphocytes as 0, 1+ and 2+ was not optimal since statistical associations with molecular and clinical variables were not as strong. We have not adjusted for multiple comparisons since the purpose of the analysis was to identify common molecular alterations in GBM related to the immune response for future tissue-based analyses. However, our analysis was limited to alterations known as significant and recurrent events in GBM pathogenesis. Furthermore, we are encouraged that each statistically significant association has a biologic rationale. Finally, this classification does not account for the functional activity of lymphocytes or specific lymphocyte subsets. While effector lymphocytes are thought to mediate the anti-tumor response, regulatory lymphocytes may suppress the cytotoxic activity of effector lymphocytes. Thus, effector and regulatory lymphocytes may have distinct molecular and histologic associations. Future studies that examine the molecular correlates of lymphocyte subsets will add substantially to the field of immunotherapy.

## Acknowledgments

The authors would like to thank the Research Pathology Lab of the Cancer Tissue and Pathology Shared Resource within the Winship Cancer Institute for their assistance with whole slide scanning and digital pathology, especially Candace Chisolm. The authors would also like to thank the leadership and support staff of the TCGA Working Group and Expert Pathology Committee for their assistance in the generation of publicly available data.

### FUNDING

This work was supported by US Public Health Service grants from the Clinical and Translational Science Award program, NIH, NCRR UL RR025008, TL1 RR025010; the In Silico Center for Brain Tumor Research Contract ST12-1100 (NCI-SAIC Frederick); and the Winship Cancer Center Support Grant (P30 CA138292).

## REFERENCES

1. Stupp R, Mason WP, van den Bent MJ, Weller M, Fisher B, Taphoorn MJ, et al. Radiotherapy plus concomitant and adjuvant temozolomide for glioblastoma. *N Engl J Med.* 2005; 352:987–996. [PubMed: 15758009]
2. Comprehensive genomic characterization defines human glioblastoma genes and core pathways. *Nature.* 2008; 455:1061–1068. [PubMed: 18772890]
3. Verhaak RG, Hoadley KA, Purdom E, Wang V, Qi Y, Wilkerson MD, et al. Integrated genomic analysis identifies clinically relevant subtypes of glioblastoma characterized by abnormalities in *PDGFRA*, *IDH1*, *EGFR*, and *NF1*. *Cancer Cell.* 2010; 17:98–110. [PubMed: 20129251]
4. Phillips HS, Kharbanda S, Chen R, Forrest WF, Soriano RH, Wu TD, et al. Molecular subclasses of high-grade glioma predict prognosis, delineate a pattern of disease progression, and resemble stages in neurogenesis. *Cancer Cell.* 2006; 9:157–173. [PubMed: 16530701]

5. Hodi FS, O'Day SJ, McDermott DF, Weber RW, Sosman JA, Haanen JB, et al. Improved survival with ipilimumab in patients with metastatic melanoma. *N Engl J Med*. 2010; 363:711–723. [PubMed: 20525992]
6. Kantoff PW, Higano CS, Shore ND, Berger ER, Small EJ, Penson DF, et al. Sipuleucel-T immunotherapy for castration-resistant prostate cancer. *N Engl J Med*. 2010; 363:411–422. [PubMed: 20818862]
7. Heimberger AB, Sampson JH. Immunotherapy coming of age: what will it take to make it standard of care for glioblastoma? *Neuro Oncol*. 2011; 13:3–13. [PubMed: 21149252]
8. Clark WH Jr, Elder DE, Guerry Dt, Braitman LE, Trock BJ, Schultz D, et al. Model predicting survival in stage I melanoma based on tumor progression. *J Natl Cancer Inst*. 1989; 81:1893–1904. [PubMed: 2593166]
9. Clemente CG, Mihm MC Jr, Bufalino R, Zurrida S, Collini P, Cascinelli N. Prognostic value of tumor infiltrating lymphocytes in the vertical growth phase of primary cutaneous melanoma. *Cancer*. 1996; 77:1303–1310. [PubMed: 8608507]
10. Dunn GP, Dunn IF, Curry WT. Focus on TILs: Prognostic significance of tumor infiltrating lymphocytes in human glioma. *Cancer Immun*. 2007; 7:12. [PubMed: 17691714]
11. Laghi L, Bianchi P, Grizzi F, Malesci A. How dense, how intense? Role of tumour-infiltrating lymphocytes across colorectal cancer stages. Re: Noshio et al. Tumour-infiltrating T-cell subsets, molecular changes in colorectal cancer, and prognosis: cohort study and literature review. *J Pathol*. 2010; 222:350–366. *J Pathol*. 2011. [PubMed: 20927778]
12. Menon AG, Janssen-van Rhijn CM, Morreau H, Putter H, Tollenaar RA, van de Velde CJ, et al. Immune system and prognosis in colorectal cancer: a detailed immunohistochemical analysis. *Lab Invest*. 2004; 84:493–501. [PubMed: 14968119]
13. Ropponen KM, Eskelinen MJ, Lipponen PK, Alhava E, Kosma VM. Prognostic value of tumour-infiltrating lymphocytes (TILs) in colorectal cancer. *J Pathol*. 1997; 182:318–324. [PubMed: 9349235]
14. Noshio K, Baba Y, Tanaka N, Shima K, Hayashi M, Meyerhardt JA, et al. Tumour-infiltrating T-cell subsets, molecular changes in colorectal cancer, and prognosis: cohort study and literature review. *J Pathol*. 2010; 222:350–366. [PubMed: 20927778]
15. Galon J, Costes A, Sanchez-Cabo F, Kirilovsky A, Mlecnik B, Lagorce-Pages C, et al. Type, density, and location of immune cells within human colorectal tumors predict clinical outcome. *Science*. 2006; 313:1960–1964. [PubMed: 17008531]
16. Zhang L, Conejo-Garcia JR, Katsaros D, Gimotty PA, Massobrio M, Regnani G, et al. Intratumoral T cells, recurrence, and survival in epithelial ovarian cancer. *N Engl J Med*. 2003; 348:203–213. [PubMed: 12529460]
17. Curiel TJ, Coukos G, Zou L, Alvarez X, Cheng P, Mottram P, et al. Specific recruitment of regulatory T cells in ovarian carcinoma fosters immune privilege and predicts reduced survival. *Nat Med*. 2004; 10:942–949. [PubMed: 15322536]
18. Yang I, Tihan T, Han SJ, Wrench MR, Wiencke J, Sughrue ME, et al. CD8+ T-cell infiltrate in newly diagnosed glioblastoma is associated with long-term survival. *J Clin Neurosci*. 2010; 17:1381–1385. [PubMed: 20727764]
19. Safdari H, Hochberg FH, Richardson EP Jr. Prognostic value of round cell (lymphocyte) infiltration in malignant gliomas. *Surg Neurol*. 1985; 23:221–226. [PubMed: 2983448]
20. Rossi ML, Jones NR, Candy E, Nicoll JA, Compton JS, Hughes JT, et al. The mononuclear cell infiltrate compared with survival in high-grade astrocytomas. *Acta Neuropathol*. 1989; 78:189–193. [PubMed: 2750489]
21. Heimberger AB, Abou-Ghazal M, Reina-Ortiz C, Yang DS, Sun W, Qiao W, et al. Incidence and prognostic impact of FoxP3+ regulatory T cells in human gliomas. *Clin Cancer Res*. 2008; 14:5166–5172. [PubMed: 18698034]
22. Parsa AT, Waldron JS, Panner A, Crane CA, Parney IF, Barry JJ, et al. Loss of tumor suppressor PTEN function increases B7-H1 expression and immunoresistance in glioma. *Nat Med*. 2007; 13:84–88. [PubMed: 17159987]

23. Fecci PE, Ochiai H, Mitchell DA, Grossi PM, Sweeney AE, Archer GE, et al. Systemic CTLA-4 blockade ameliorates glioma-induced changes to the CD4+ T cell compartment without affecting regulatory T-cell function. *Clin Cancer Res.* 2007; 13:2158–2167. [PubMed: 17404100]
24. Fecci PE, Mitchell DA, Whitesides JF, Xie W, Friedman AH, Archer GE, et al. Increased regulatory T-cell fraction amidst a diminished CD4 compartment explains cellular immune defects in patients with malignant glioma. *Cancer Res.* 2006; 66:3294–3302. [PubMed: 16540683]
25. Cerami E, Gao J, Dogrusoz U, Gross BE, Sumer SO, Aksoy BA, et al. The cBio cancer genomics portal: an open platform for exploring multidimensional cancer genomics data. *Cancer Discov.* 2012; 2:401–404. [PubMed: 22588877]
26. Parsons DW, Jones S, Zhang X, Lin JC, Leary RJ, Angenendt P, et al. An integrated genomic analysis of human glioblastoma multiforme. *Science.* 2008; 321:1807–1812. [PubMed: 18772396]
27. Noushmehr H, Weisenberger DJ, Diefes K, Phillips HS, Pujara K, Berman BP, et al. Identification of a CpG island methylator phenotype that defines a distinct subgroup of glioma. *Cancer Cell.* 2010; 17:510–522. [PubMed: 20399149]
28. Turcan S, Rohle D, Goenka A, Walsh LA, Fang F, Yilmaz E, et al. IDH1 mutation is sufficient to establish the glioma hypermethylator phenotype. *Nature.* 2012; 483:479–483. [PubMed: 22343889]
29. Yan H, Parsons DW, Jin G, McLendon R, Rasheed BA, Yuan W, et al. IDH1 and IDH2 mutations in gliomas. *N Engl J Med.* 2009; 360:765–773. [PubMed: 19228619]
30. Prins RM, Soto H, Konkankit V, Odesa SK, Eskin A, Yong WH, et al. Gene expression profile correlates with T-cell infiltration and relative survival in glioblastoma patients vaccinated with dendritic cell immunotherapy. *Clin Cancer Res.* 2011; 17:1603–1615. [PubMed: 21135147]
31. Cooper LA, Gutman DA, Chisolm C, Appin C, Kong J, Rong Y, et al. The tumor microenvironment strongly impacts master transcriptional regulators and gene expression class of glioblastoma. *Am J Pathol.* 2012; 180:2108–2119. [PubMed: 22440258]
32. Reis RM, Konu-Lebleblicioglu D, Lopes JM, Kleihues P, Ohgaki H. Genetic profile of gliosarcomas. *Am J Pathol.* 2000; 156:425–432. [PubMed: 10666371]
33. Meyer-Puttlitz B, Hayashi Y, Waha A, Rollbrocker B, Bostrom J, Wiestler OD, et al. Molecular genetic analysis of giant cell glioblastomas. *Am J Pathol.* 1997; 151:853–157. [PubMed: 9284834]
34. Watanabe K, Peraud A, Gratas C, Wakai S, Kleihues P, Ohgaki H. p53 and PTEN gene mutations in gemistocytic astrocytomas. *Acta Neuropathol.* 1998; 95:559–564. [PubMed: 9650746]
35. Burger PC, Pearl DK, Aldape K, Yates AJ, Scheithauer BW, Passe SM, et al. Small cell architecture—a histological equivalent of EGFR amplification in glioblastoma multiforme? *J Neuropathol Exp Neurol.* 2001; 60:1099–1104. [PubMed: 11706939]
36. Pollack BP, Sapkota B, Cartee TV. Epidermal growth factor receptor inhibition augments the expression of MHC class I and II genes. *Clin Cancer Res.* 2011; 17:4400–4413. [PubMed: 21586626]

### Statement of Translational Relevance

Tumor-infiltrating lymphocytes (TILs) are present in a subset of GBMs, suggesting some are more capable of eliciting an adaptive immune response. We hypothesized TILs are differentially distributed among specific molecular classes of GBM and used histologic data linked to multiplatform molecular analysis from The Cancer Genome Atlas (TCGA) to identify correlates. We have shown that TILs are associated with specific genomic alterations and related to transcriptional class, which may provide insight into the biologic significance of TILs in GBM and predict response to immunotherapy.

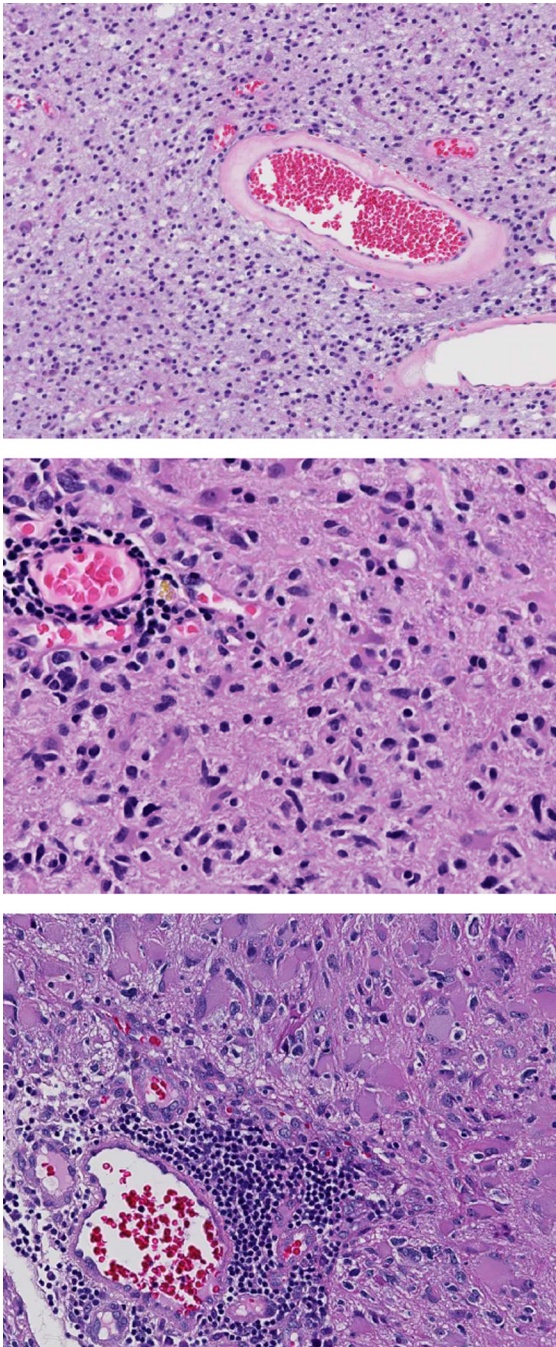


**Figure 1.** Representative examples of permanent section histologic slides from TCGA cases. Lymphocytes were identified as small round cells with scant cytoplasm and darkly staining nuclei. Cases with a complete absence of lymphocytes were labeled 0 (absent) (top). Cases with lymphocytes present in <50% of tumor tissue were categorized 1+ (present) (middle). Cases with lymphocytes present in  $\geq$  50% were categorized 2+ (abundant) (bottom).

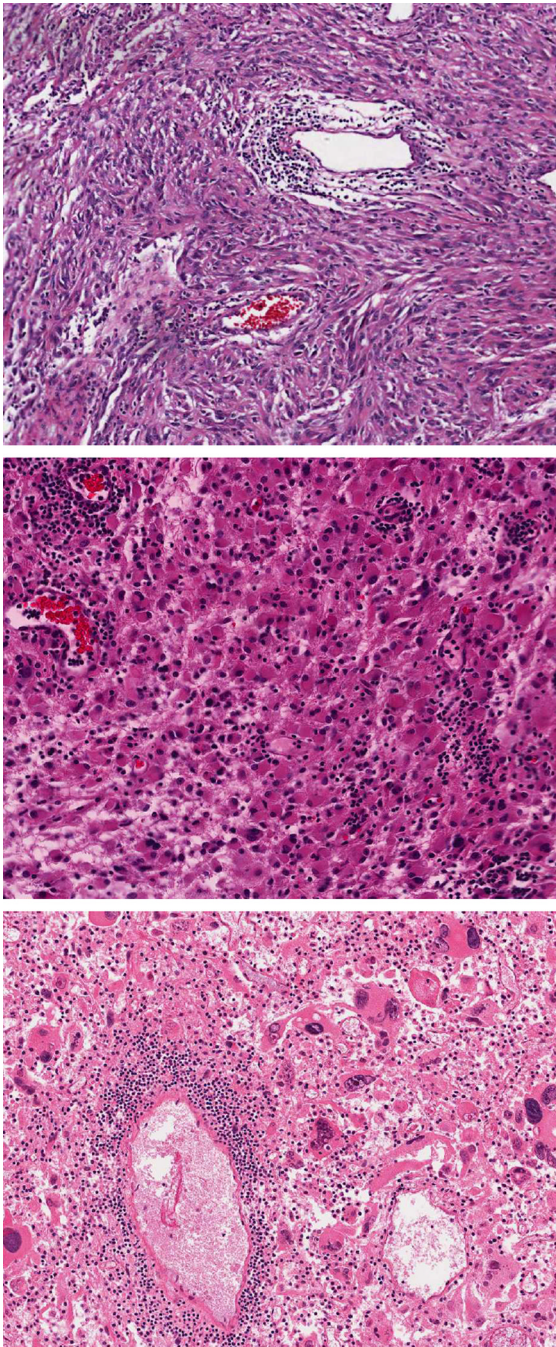


**Figure 2.** Representative examples of GBM morphologic subtypes associated with the presence of lymphocytes in TCGA permanent section histologic slides. TILs are enriched in GBMs with sarcomatous cells (top), gemistocytes (middle) and giant cells (bottom).

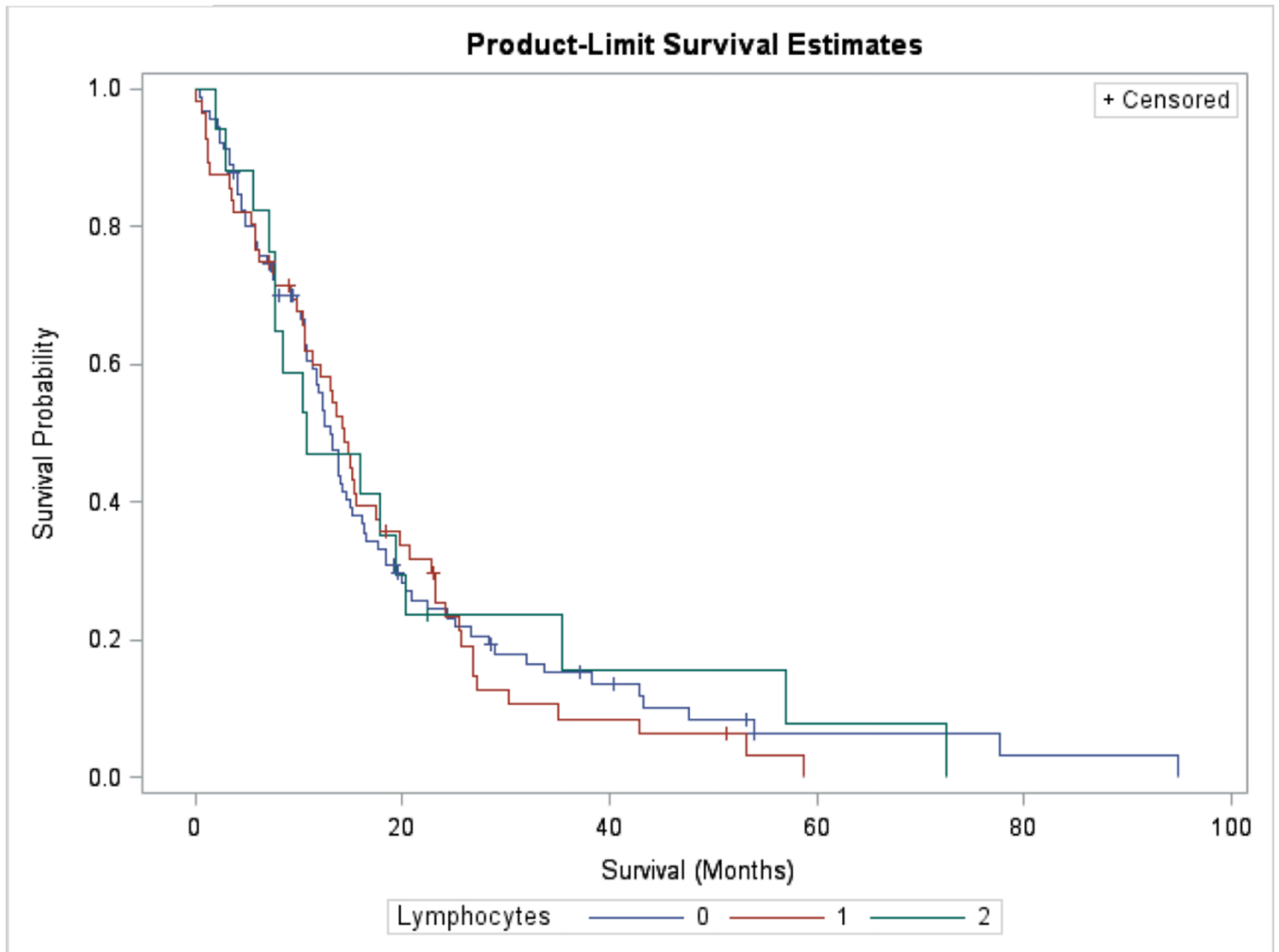


**Figure 3.** Kaplan–Meier estimates of survival according to absent (0), present (1+) or abundant (2+) lymphocytes. TILs are not associated with improved survival (log-rank  $p>0.05$ ).

**Table 1**

18 histopathologic features were categorized as absent (0), present (1+), or abundant (2+) in 171 TCGA GBMs. TILs are associated with specific histopathologic features in GBM.

Histopathologic Feature	Mantel-Haenzel chi-square p-value	Spearman correlation
Inflammation	<0.001	0.93
Pseudopalisading necrosis	0.01	-0.19
Zonal necrosis	0.04	0.16
Neutrophils	0.09	0.13
Macrophages	<0.001	0.32
Microvascular hyperplasia	0.59	-0.04
Endothelial hyperplasia	0.05	-0.15
Epithelial metaplasia	0.04	0.16
Gemistocytes	0.01	0.22
Giant cells	0.02	0.18
Oligodendroglial cells	0.01	-0.19
Sarcomatous metaplasia	<0.01	0.22
Small cells	<0.01	-0.24
Mineralization	0.68	0.03
Satellitosis	0.20	-0.10
White matter invasion	0.09	-0.13
Cortex invasion	0.71	-0.03

Mantel-Haenzel chi-square test and Spearman correlation were used to examine associations between lymphocytes (0, 1+, 2+) and other histopathologic features (0, 1+, 2+)

Mantel-Haenzel exact chi-square test was used when 25% of the cells had <5 observations

Effective Sample Size 171



**Table 2**

TILs are associated with specific mutations in GBM

Gene	n	Chi square p-value (0, 1+, 2+)	Chi square p-value (0 vs 1+, 2+ combined)	Chi square p-value (0, 1+ combined vs 2+)
TP53	33	0.13	0.06	0.15
PTEN	29	0.15	0.06	0.44
EGFR	26	0.82	0.54	1.00
NF1	16	<b>0.03</b>	0.74	<b>0.04</b>
RB1	10	<b>0.04</b>	<b>0.04</b>	0.22
PIK3R1	9	0.67	0.49	1.00
PIK3CA	7	0.72	1.00	0.50
IDH1	4	0.53	1.00	0.32
ERBB2	0	-	-	-

Chi-square test was used to examine associations between lymphocytes (0, 1+, 2+) and mutations (0, 1)

Fisher's exact test was used when 25% of the cells had <5 observations

Effective Sample Size 99

Categories were combined to identify associations driven by cases with either complete absence or abundance of lymphocytes

**Table 3**

TILs are depleted in *EGFR*-amplified and homozygous *PTEN*-deleted tumors

CNA	(%)	Chi square p-value (0, 1+, 2+)	Chi square p-value (0 vs 1+, 2+ combined)	Chi square p-value (0, 1+ combined vs 2+)
<b>Amplifications</b>				
EGFR	49.3	<b>0.05</b>	<b>0.04</b>	0.06
CDK4	14.5	0.37	0.22	0.47
PDGFRA	14.1	0.61	0.73	0.47
MDM4	9.9	0.23	0.24	0.64
MDM2	9.3	0.81	0.82	1.00
MET	8.8	0.57	0.79	0.48
CDK6	7.0	0.75	0.65	0.69
CCND2	4.0	1.00	1.00	1.00
AKT3	3.2	1.00	1.00	1.00
MYCN	2.6	1.00	0.62	1.00
PIK3CA	2.4	0.69	0.60	1.00
<b>Deletions</b>				
CDKN2A	62.0	0.23	0.09	0.48
CDKN2B	61.0	0.23	0.09	0.48
PTEN	10.3	0.09	<b>0.03</b>	0.69
RB1	3.6	0.87	1.00	0.57
CDKN2C	3.6	0.71	1.00	0.51
PARK2	2.0	1.00	1.00	1.00
NF1	1.2	0.07	0.10	0.30

Chi-square test was used to examine associations between lymphocytes (0, 1+, 2+) and CNAs

Fisher's exact test was used when 25% of the cells had <5 observations

Effective Sample Size 153

Categories were combined to identify associations driven by cases with either complete absence or abundance of lymphocytes

**Table 4**

TILs are enriched in the mesenchymal class and depleted in the classical class

Lymphocytes	Transcriptional Class				Total
	Classical	Mesenchymal	Neural	Proneural	
0	31	27	13	19	90
1+	10	18	9	18	55
2+	1	12	2	2	17
Total	42	57	24	39	162

Chi-square test was used to examine associations between lymphocytes (0, 1+, 2+) and transcriptional class

Fisher's exact test was used when 25% of the cells had <5 observations

Effective sample size 162